EasyChair Preprint

№ 10429

Power Generation Prediction of a New Tower Type Thermal/Photovoltaic (T/PV) Power Generation System Based on Spectral Beam Splitting

Zhongzhu Qiu, Xingrui Ni, Qunzhi Zhu, Yongjian Ye, Tao Zhang, Jingyong Cai, Ning Xu, Miaomiao Zhang and Chengyang Li

June 30, 2023

Power Generation Prediction of A New Tower Type Thermal/Photovoltaic(T/PV) Power Generation System Based on Spectral Beam Splitting

Zhongzhu Qiu[1], Xingrui Ni[2], Qunzhi Zhu[3], Yongjian Ye[4], Tao Zhang[5], Jingyong Cai[6], Ning Xu[7], Miaomiao Zhang[8], Chengyang Li[9]

[1] *Shanghai University of Electric Power, Shanghai, China, qiuzhongzhu@shiep.edu.cn*

[2] *Shanghai University of Electric Power, Shanghai, China, 1181579260@qq.com*

[3] *Shanghai University of Electric Power, Shanghai, China, zhuqunzhi@shiep.edu.cn*

[4] *East China Electric Power Design Institute Co., Ltd. of China Power Engineering Consulting group, Shanghai, China, yyj1@ecepdi.com*

[5] *Shanghai University of Electric Power, Shanghai, China, taozhang@shiep.edu.cn*

[6] *Shanghai University of Electric Power, Shanghai, China, caijingyong@126.com*

[7] *Shanghai University of Electric Power, Shanghai, China, suepxn@163.com*

[8] *Shanghai University of Electric Power, Shanghai, China, 184790618@qq.com*

[9] *Shanghai University of Electric Power, Shanghai, China, 2111270992@qq.com*

Abstract: *At present, photovoltaic power generation can only utilize a portion of the solar band, and the remaining bands entering the battery will not be used for power generation, but will instead increase the temperature of the battery, leading to a decrease in photoelectric conversion efficiency. Therefore, using frequency division to utilize some photons that do not respond to the battery for thermal utilization can effectively improve the energy conversion efficiency of solar energy. In this article, the author proposes a tower-type thermal/photovoltaic (T/PV) power generation system using spectral beam splitting technology. The spectroscopic glass is formed by plating a layer of spectral selective film on the surface of special glass, and then install the spectroscopic glass as a cover plate on the photovoltaic cell to replace the heliostat in the tower thermal power generation,so that specific wavebands enter the photovoltaic cell through the spectroscopic glass for photovoltaic power generation, and other wavebands are reflected onto the collector for thermal power generation. The mirror field arrangement was designed using the MUUEN algorithm, and the proposed system was analyzed optically and thermodynamically at the AM1.5D solar spectrum as the incident irradiance flux density. Solar radiation data for a typical meteorological year were used to forecast and compare the full-year power generation of photovoltaic power, solar thermal power and this system. The results show that the combined power production of the tower-type* T/PV power generation system based on spectral beam splitting *is higher than the other two systems under the selected climatic conditions.*

Keywords: *solar energy; power generation system; solar tower; beam splitting technology; thermodynamic analy*

1. INTRODUCTION

Solar energy is inexhaustible as well as clean and free of charge, making it a unique advantage and a huge potential for development and utilization. At present, the utilization of solar energy mainly includes thermal utilization and light utilization, where thermal utilization mainly includes solar water heater, solar thermal power generation and high temperature solar furnace, while light utilization is mainly photovoltaic power generation(Li, 2022). Solar thermal power generation in thermal utilization is the focusing of solar radiation, using heat collection and heat exchange equipment to transfer heat to thermal fluid, and the thermal fluid drives the thermal machine to generate electricity. Solar thermal power generation is mainly divided into trough type, tower type and dish type according to the different forms of solar energy concentration. However, the annual power generation efficiency of this type of concentrating solar thermal power generation is only 11-25 %, while the tower power generation technology has higher concentrating multiplier, easier to reach higher working temperature, and higher thermal conversion efficiency, which makes it have more room for improvement(O'neill, 2021). Today, photovoltaic power generation in the laboratory is capable of converting about 30% of simulated sunlight into electricity(Ju et al., 2012), while in engineering this efficiency is even lower, at 16-20 %(Zhang, 2019). However, due to the characteristics of photovoltaic power generation, only a specific spectral range of solar radiation can be converted into electricity, the rest of the band is not only not conducive to photovoltaic power generation, but will lead to an increase in cell temperature and thus reduce the efficiency of power generation.

In order to fully utilize solar energy in a wider range of solar spectral wavelengths, the concept of T/PV power generation system based on spectral beam splitting was proposed, i.e., a specific spectral range for photovoltaic power generation and other spectral ranges for photothermal power generation(Ju et al., 2017). Mahmoudinezhad et al. (2022) built a simple hybrid photovoltaic-thermoelectric generator beam splitter (PV-TEG-BS) system using photovoltaic cells, a temperature differential generator, and a beam splitter for spectral splitting. Experimentally, it was found that the use of the spectral beam splitting technique reduces the power generation of the solar thermal component but significantly increases the power generation of the PV cells in the system, and the total power generation of the system is also higher. In order to scale up the system and utilization efficiency, numerous scholars have tried to replace the temperature difference generator in the system with concentrated solar thermal power technology. Widyolar, Jiang and Winston (2018), Jiang et al. (2009), Liu et al. (2014), Segal, Epstein and Yogev (2004) combined trough, butterfly, linear Fresnel and tower with a split-spectrum photothermal -photovoltaic composite power system. The simulation results show that the power generation efficiency of the system is all improved than before. However, most of the current tower type T/PV power generation system based on spectral beam splitting are set up with a selective transmission mirror in the path of the sunlight reflected by the heliostat to the collector, so that the specified waveband reflection is used for photovoltaic power generation and the other wavebands are used for solar thermal power generation. However, this structure leads to increased path loss of sunlight and the construction difficulty of setting up a mirror surface between the heliostat and the collector is also relatively high.

Therefore, In this article, the author proposes a new tower type T/PV power generation system system based on spectral beam splitting. The system design is based on a spectral glass that is capable of transmitting completely in the specified wavelength band and reflecting completely in other wavelength bands. By combining the spectroscopic glass with the solar panel to form a spectroscopic photovoltaic panel and replacing the heliostat in a conventional tower-type solar thermal power system, the path loss of sunlight is reduced. After designing the arrangement of the mirror field, the optical and thermodynamic analysis of the system is carried out, and the power generation capacity of the system is estimated for each month of the year based on the meteorological data of a typical meteorological year in Lhasa, and compared with conventional photovoltaic power generation and conventional tower-type thermal power generation.

2. A NEW TOWER-TYPE T/PV POWER GENERATION SYSTEM BASED ON SPECTRAL BEAM SPLITTING

2.1. Structure of tower-type T/PV power generation system based on spectral beam splitting

In this paper, the authors constructed a new tower-type T/PV power generation system based on spectral beam splitting as shown in Figure 1. Combining a spectral glass with a photovoltaic cell to replace the heliostat in a tower-type thermal power generation heliostat field allows specific wavelengths to pass through the spectral glass into the photovoltaic cell for photovoltaic power generation and other wavelengths to be reflected onto the collector for thermal power generation.

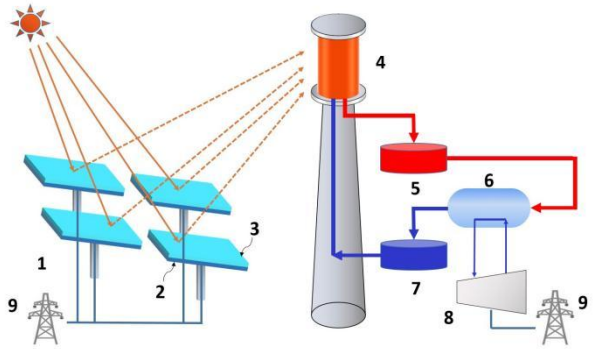

1.Heliostats field 2.PV 3.Spectroscopic glass 4.Collector 5.Hot Salt Shaker 6.Steam generator 7.Cold salt tank 8.Steam turbine 9.On-grid

Figure 1: Construction of tower-type T/PV hybrid system based on spectral beam splitting

2.2. Spectral photovoltaic panels

A spectrally selective thin film is coated on the surface of the special glass to form a spectroscopic glass, and then the spectroscopic glass is mounted on the conventional solar panel as a cover to assemble a PV panel based on spectral beam splitting(SBS PV panel). The structure of the SBS PV panel is shown in Figure 2, and the materials of each layer from top to bottom are spectroscopic glass, first EVA sheet, conductive welding tape, cell, second EVA sheet and TPT backsheet.

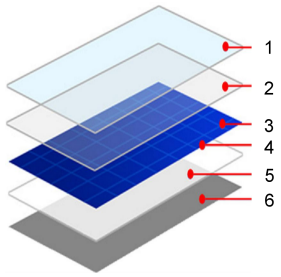

1.Spectroscopic glass 2.First EVA board 3.Conductive welding tape 4.Cell 5.Second EVA board 6.TPT backplane

Figure 2: Structure of SBS PV panel

The photovoltaic cells in the SBS PV panels use monocrystalline silicon (c-Si) solar cells with a spectrally selective coating with a theoretical spectral reflectance of (Wang et al., 2019):

Equation 1: Theoretical spectral reflectance of coatings

$$\rho(\lambda) = \begin{cases} 0 & (500nm \le \lambda \le 900nm) \\ 1 & (\lambda \le 500nm, \lambda > 900nm) \end{cases}$$

Where:

- λ = wavelength of solar radiation (nm)

2.3. Arrangement of the heliostat field

In this study, the conventional radial interleaved layout is chosen for the heliostat field layout, which can effectively reduce the shadowing and occlusion loss of the heliostat field, and then an unobstructed heliostat field layout is established using the MUUEN algorithm (Siala and Elayeb, 2001).

The conventional radially staggered layout is shown in Figure 3, where the heliostats are distributed in concentric rings centered on the heat collection tower, and the distribution of the heliostats is centrosymmetric. The small circles distributed on each ring represent a heliostat. The intersection of the ring and the north axis is called the essential rings when there is a heliostat, and the intersection is called the staggered ring when there is no heliostat. The characteristic diameter DM of the heliostat is is equal to the diagonal of the heliostat plus the separation distance：

Equation 2: Characteristic diameter of heliostat

$$DM = l_m(\sqrt{1+f^2} + dS)$$

Where,

- l_m = heliostat length (m)
- f = heliostat width-to-length ratio
- dS = ratio of heliostat separation distance to heliostat length

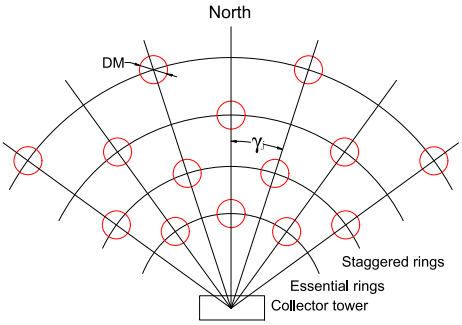

Figure 3: Traditional radial staggered layout

For no blocking, the minimum characteristic diameter DM_{min} of a square heliostat is (Collado and Turégano, 1989):

Equation 3: Minimum characteristic diameter of heliostat

$$DM = 2w_m$$

Where,

- w_m = heliostat width (m)

Angular direction unit: The angle between the distribution axes. In radians, this is given by:

Equation 4: The angle between the distribution axes

$$\gamma_j = \frac{DM}{2R_0}$$

Where,

- R_0 = radius of the first ring (m)

The radius of the first circle in the heliostat column is given by:

Equation 5: Radius of the first ring

$$R_0 = R_{min} = 0.75 * H_t$$

Where,

- H_t = aim point height

Angular direction: The angle between the north axis and distribution axes. It is given by:

Equation 6: Angular direction

$$\Psi = \pm n\gamma_j$$

Where,

- n = 0,2,... for essential rings,
- n = 1,3,... for staggered rings

For no blocking radially staggered distribution the radius of the circle is designed as shown in Figure 4.

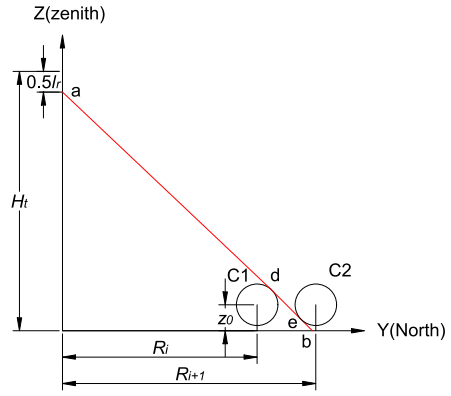

Figure 4: Schematic Diagram of No Blocking Radial Staggered Distribution

The radius of any other ring in the field is determined in accordance with the graphical field layout method. In Figure 4, C1 represents the front view of a known heliostat from the previous ring and ab represents the lowest limit of reflected rays originating behind C1 and striking the receiver with no blocking by C1. Then, the radius of the new ring, equal to R_{i+1}, is obtained by solving the equations of the line ab and circles C1 and C2.

The radius of each circle R_i on the horizontal surface can be solved by the geometric relationship shown in Figure 4. After obtaining the radius of each circle, the angle of the adjacent distribution axis, The coordinates of a single heliostat can be expressed as :

Equation 7: Coordinates of each heliostat

$$x_m = R_i sin\Psi_m$$
$$y_m = R_i cos\Psi_m$$
$$z_m = z_0$$

In this paper, we assume that the height of the collector tower is 50 m, the length of both sides of the heliostat is 4 m, the height is 5 m, and the solar receiving angle of the collector tower is 90°. Under this condition, the efficiency of using the MUUEN algorithm is relatively high (Barberena et al., 2016). Using the above equation, the heliostats field arrangement can be calculated as shown in Figure 5. Each circle in the figure represents a fixed heliostat, with the positive x-axis pointing due east and the positive y-axis square pointing due north.

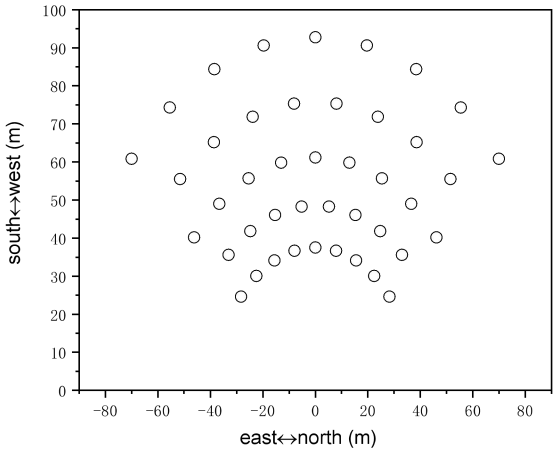

Figure 5: Heliostat field layout

3. MATHEMATICAL MODEL OF SYSTEM'S POWER GENERATION FORECAST

3.1. Photovoltaic power generation mathematical model

For a tower-type T/PV hybrid system based on spectral beam splitting, the maximum power generated by the solar cells can be expressed as (Wang, 2022):

Equation 8: The maximum power generated by the solar cells

$$P_{PV,BS} = V_{OC,BS} \cdot I_{SC,BS} \cdot FF$$

Where,

- $V_{OC,BS}$ = open circuit voltage (V)
- $I_{SC,BS}$ = short circuit current (A)
- FF = fill factor

The open circuit voltage $V_{OC,BS}$, short circuit current $I_{SC,BS}$ and fill factor FF of the solar cell in the system under λ_1-λ_2 band are given by:

Equation 9: Open circuit voltage

$$V_{OC,BS} = \frac{hc}{\lambda_2} \cdot \frac{V_{OC}}{E_g}$$

Equation 10: Circuit current

$$I_{SC,BS} = \int_0^{\infty} \tau(\lambda) \cdot E(\lambda) \cdot QE(\lambda) \cdot \frac{e\lambda}{hc} d\lambda$$

Equation 11: Fill factor

$$FF = \frac{v_{OC} - ln(v_{OC} + 0.72)}{1 + v_{OC}}(1 - R_S)$$

Where,

- h = planck constant (6.626×10^{-23})
- c = velocity of light in the vacuum (3×10^8 m/s)
- V_{OC} = open circuit voltage of the solar cell under 1 × SUN illumination condition (V)
- Eg = bandgap energy of solar cell (1.4 eV)
- τ(λ) = spectral transmissivity of spectral photovoltaic panel
- E(λ) = incident spectral irradiance at AM1.5D
- QE(λ) = spectral external quantum efficiency of solar cells
- e = charge of an electron (1.6×10^{-19} C)
- v_{oc} = open circuit voltage normalized to the thermal voltage V_{th}

- R_S = actual solar cell series resistance

The thermal voltage V_{th} can be expressed as:

Equation 12: Thermal voltage

$$V_{th} = \frac{\eta_f kT}{e}$$

Where,

- η_f = diode ideality factor
- k = boltzmann constant (1.38065×10^{-23} $m^2kg\cdot s^{-2}K^{-1}$)
- T = operating temperature of solar cell (°C)

The incident radiation received by the solar cell after spectral division $Q_{PV,BS}$ is:

Equation 13: Incident radiation received by the solar cell after spectral division

$$Q_{PV,BS} = Q_{in}\int_0^{\infty}\tau(\lambda)d\lambda$$

Equation 14: Incident solar energy flux on the solar concentrator

$$Q_{in} = \eta_{cos}\int_0^{\infty}E(\lambda)d\lambda$$

Where,

- Qin = incident radiation of the system ($KWh\cdot m^{-2}$)
- η_{cos} = cosine efficiency of the system

Thus the energy efficiency of the photovoltaic part of the tower-type hybrid system based on spectral beam splitting η_{PV} is:

Equation 15: Overall energy efficiency of the system

$$\eta_{PV} = \frac{P_{PV,BS}}{Q_Z}$$

Where,

- Q_Z = total solar radiation ($KWh\cdot m^{-2}$)

The formula for calculating the power of conventional PV panels is as follows:

Equation 16: Power of conventional PV panels

$$P_{PV} = V_{OC}\cdot I_{SC}\cdot FF$$

The short-circuit current and the solar cell efficiency is:

Equation 17: Short circuit current of traditional photovoltaic panels

$$I_{SC} = \int_0^{\infty}E(\lambda)QE(\lambda)\frac{e\lambda}{hc}d\lambda$$

Equation 18: Solar cell efficiency

$$\eta_{PV} = \frac{P_{PV}}{Q_Z}$$

Where, P_{PV}, V_{OC} and I_{SC} respectively represent the output power of the photovoltaic component without frequency division and their corresponding open circuit voltage and short circuit current values.

For a fixed inclination solar panel the received incident radiation is:

Equation 19: Incident radiation received by fixed tilt solar panels

$$Q_{in} = Q_Z\cdot\eta_{cos,pv}$$

The expression for the cosine efficiency of a fixed inclination PV panel is:

Equation 20: Cosine efficiency of a fixed-tilt PV panel

$$\eta_{cos,pv} = sin\alpha cos\beta - cos\alpha sin\beta cosA$$

Where,

- α = Solar altitude angle (°)
- β = Tilt angle of photovoltaic panels (°)
- A = Solar Azimuth (°)

The expressions for the solar altitude and azimuth angles are:

Equation 21: Solar altitude angle

$$\alpha = arcsin(sin\delta sin\phi + cos\delta cos\omega cos\phi)$$

Equation 22: Solar azimuth angles

$$A = arcsin(\frac{-cos\delta sin\omega}{cos\alpha})$$

Where,

- δ = declination angle (°)
- ϕ = latitude angle (°)
- ω = hour angle (°)

The latitude angle is usually the local latitude, the declination angle and the hour angle are calculated by the formula:

Equation 23: Declination angle

$$sin\delta = 0.39795\times cos[0.98563\times(N-173)]$$

Equation 24: Solar hour angle

$$\omega = 15\times(t_s - 12)$$

Where,

- N = the number of days into a leap year cycle with N = 1 being January 1 of each leap year
- t_s = solar time in hours (h)

After choosing the local latitude as the inclination angle, the cosine efficiency of the fixed inclination PV panel can be found for the whole year.

3.2. Mathematical model of tower hhermal power generation

The power generation capacity of the photothermal component of a tower-type T/PV hybrid system based on spectral beam splitting is usually determined by the total mirror area, solar irradiance per unit area time, optical efficiency and other influencing factors. The amount of electricity generated by the solar thermal fraction per unit area $P_{TH,BS}$ and the amount of incident radiation received by the collector $Q_{TH,BS}$ can be expressed as (Xie, 2017):

Equation 25: Electricity generated by the solar thermal fraction

$$P_{TH,BS} = Q_{TH,BS}\cdot\eta_{else}$$

Equation 26: Incident radiation received by the

$$Q_{TH,BS} = Q_{in}\cdot\int_0^{\infty}\rho(\lambda)d\lambda$$

collector

Where,

- η_{else} = other influencing factors, representing the various losses encountered in the actual operation of tower solar thermal power for example
- $\rho(\lambda)$ = spectral reflectance of the spectral photovoltaic panel

The most important factors in optical efficiency are the cosine efficiency of the heliostat and the shadowing and blocking losses. As the fixed helioscopic field is designed in this paper using the no blocking model, the shadow loss is small so it is not considered for the time being. The cosine efficiency, on the other hand, depends on the position of the solar rays and the individual heliostats relative to the receiver. Therefore, a coordinate system as shown in Figure 6 was established for calculating the cosine efficiency. The x-axis of this coordinate system points north, the y-axis points east, the collector is the coordinate origin, A is the collector coordinate, and B is the coordinate of a certain heliostat.

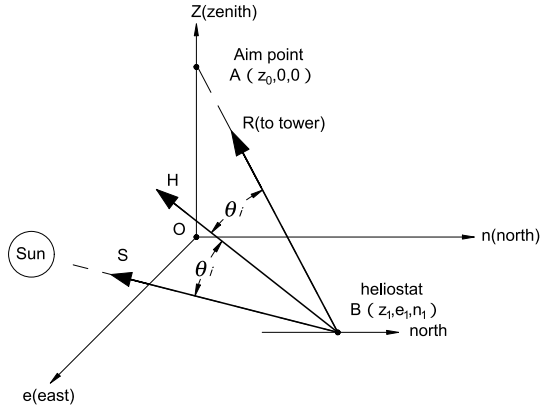

Figure 6: Coordinates of sunlight reflected by a single heliostat

The expression to calculate the cosine efficiency of the system is (Stine and Geyer, 2001):

Equation 27: Cosine efficiency of the system

$$\eta_{cos} = cos\theta_i$$

Equation 28: Angle of incidence of the sun

$$cos2\theta_i = \frac{(z_0 - z_1)sin\alpha - e_1 cos\alpha sinA - n_1 cos\alpha cosA}{\sqrt{[(z_0 - z_1)^2 + e_1^2 + n_1^2]}}$$

Where,

- θ_i = angle of incidence of sunlight (°)
- z_0 = height of collector (m)
- z_1, e_1, n_1 = coordinates of heliostat (m)

After determining the date, the time of the day, the local latitude, the collector, and the coordinates of the heliostat, the cosine efficiency of that heliostat can be found for any time of the year.

The literature (Yao, 2019) presents the estimation of power generation for the actual operation of tower solar thermal power, on the basis of which this paper assumes that the other influencing factors in the power generation process are 0.237, i.e. η=0.237.

Therefore, the efficiency of the photothermal component of the tower-type T/PV hybrid system based on spectral beam splitting $\eta_{PV,BS}$ is:

Equation 29: Efficiency of the photothermal component

$$\eta_{TH,BS} = \frac{P_{TH,BS}}{Q_Z}$$

This gives the total generation capacity P_{total} and total generation efficiency η_{sys} of the tower-type T/PV hybrid system based on spectral beam splitting as：

Equation 30: Total generation capacity of the tower-type T/PV hybrid system

$$P_{total} = P_{PV,BS} + P_{TH,BS}$$

Equation 31: Total generation efficiency of the tower-type T/PV

$$\eta_{SYS} = \frac{P_{total}}{Q_Z}$$

3.3. Model solution

In this paper, we simulate a new tower-type T/PV hybrid system based on spectral beam splitting under AM1.5D ideal spectral (ASTM international, 2012) distribution using the equations presented in the previous paper.

The model solution first requires the assumption of the spectral transmittance profile of the system, i.e., which band is selected for complete transmission for photovoltaic power generation. Using the assumed spectral transmittance curves combined with Eqs. (13) - (28), the respective incident radiation amounts of the photovoltaic and photothermal components of the system can be obtained. The model solution is then divided into two parts: photovoltaic and solar thermal.

In the photovoltaic power generation section, c-Si solar cells are selected in this paper, and their open-circuit voltage, fill factor (Green et al., 2013), diode ideality factor η_f, and series resistance R_s (Green et al., 2021) under standard test conditions are shown in Table 1. Assuming the cell temperature of 30°C, the open-circuit voltage, short-circuit current and fill factor of the PV cell after spectral separation are calculated by Eqs. (9)-(11), respectively, and then the power generation of the PV part of the system at a given spectral transmittance and the power generation efficiency are calculated using Eqs. (8) and (15).

Table 1 Thermodynamic analysis constants

Parameters		Parameters	
Voc	0.7485	η_f	1.28
FF	0.855	R_s	0.012

In the solar thermal power generation section, Lhasa is

chosen as the simulation site, and the solar altitude angle, solar azimuth angle, declination angle and hour angle of a single spectral photovoltaic panel can be calculated for each moment of the year using Eqs. (21)-(24). Based on the mirror field arrangement layout designed in Section 2.3 to obtain the relative coordinates between each spectral PV panel and the collector, the cosine efficiency of the mirror field can be calculated using Eq. (28). Using Eqs. (25) and (29), the amount of power generated by the photothermal part of the system for a given spectral transmittance and the power generation efficiency can be calculated. Finally, the total generation capacity and total generation efficiency of the tower-type split-spectrum composite power generation system are obtained using Eqs. (30) and (31). The solution process is shown in Figure 7.

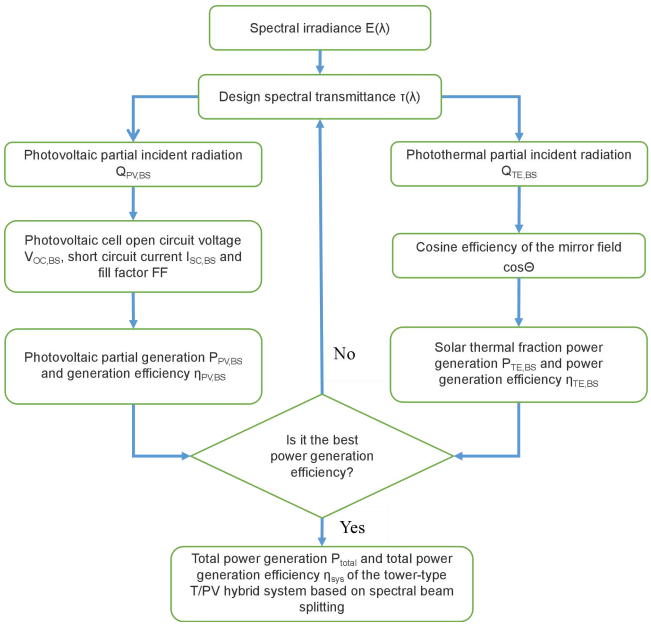

Figure 7: Solution process diagram of tower type hybrid power generation system based on spectral beam splitting

As shown in Figure 8, setting different spectral transmittance bands can calculate the total power generation efficiency of different tower-type T/PV power generation system based on spectral beam splitting. It can be seen that the total power generation efficiency of the system is highest when the starting band is 500 nm and the ending band is 900 nm, which is 21.31 %.

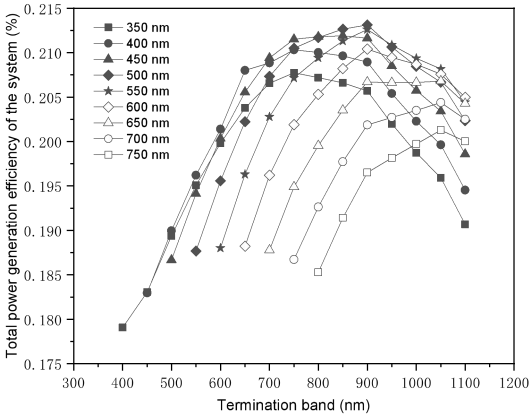

Figure 8: Total power generation efficiency of the system at different wavebands

When the starting band is 500-900 nm, the ideal spectral distribution of AM1.5D on the surface of the PV cell and collector after spectroscopic glass spectroscopy and the frequency division band are shown in Figure 9, and the total incident radiation on the surface of the spectroscopic glass can be obtained as 1000.37 W/m^2 by integrating the curve. The incident radiation received by the solar cell surface is 490.18 W/m^2 and the incident radiation reflected to the collector is 510.19 W/m^2. The average transmittance of the spectroscopic glass is 49.08 % and the average reflectance is 50.92 %.

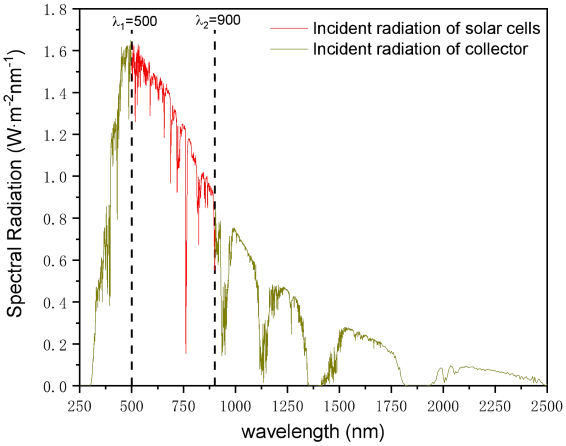

Figure 9: Spectral distribution of incident radiation

The quantum efficiency of c-Si solar cells versus the optimal spectral transmittance curve of the spectroscopic glass is shown in Figure 10. When the starting band is 500-900 nm, the power generation efficiency of the photovoltaic part of the tower-type T/PV power generation system is 33.17 %. By using Eqs. (16)-(19), it can be calculated that the power generation efficiency is 25.06 % when direct sunlight hits the photovoltaic panel, and the power generation efficiency of this c-Si solar cell given in the literature (Green et al., 2021) is 25.3±0.4 %, which is consistent with the power generation efficiency calculated in this paper.

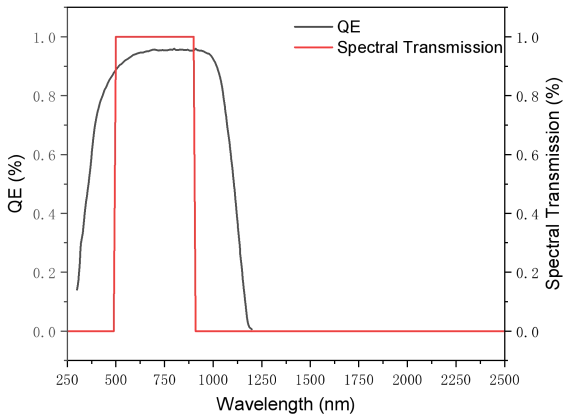

Figure 10: Quantum efficiency and spectral transmittance curves of c-Si solar cells versus spectroscopic glass

4. RESULTS AND DISCUSSION

The total system power generation corresponding to different bands in the AM1.5D solar spectrum irradiation as defined by ASTM G173-03 (2012) can be obtained for the tower-type T/PV power generation system based on spectral beam splitting according to the equation given in the third part. This paper uses the solar direct radiation data in a typical meteorological year in Lhasa as the basis, assuming that the trend of direct radiation with wavelength in it is the same as the solar spectrum of AM1.5D, and the total power generation under each moment of the year when the system is in Lhasa can be calculated by the same way.

The month-by-month values of direct radiation for a typical meteorological year in Lhasa are shown in Figure 11, where the average value of the three months with the least direct radiation is 142.9 KWh/m^2, which is 72.60 % of the average value of the three months with the most total radiation of 196.8 KWh/m^2. It can be seen that the radiation levels in Lhasa do not vary much from season to season throughout the year, while the total radiation level is higher in summer due to the long sunshine hours.

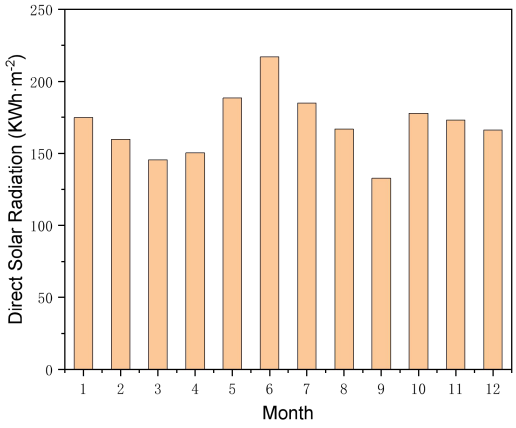

Figure 11: Monthly value of direct radiation

Bringing the data of direct radiation to Eqs. (26) and (27) gives the cosine efficiency of the spectral PV panel at each moment of the year for a given coordinate. Based on the coordinates of each mirror in the mirror field designed in section 2.3, the total incident radiation per unit area received by the mirror field can be calculated. The average cosine efficiency of the mirror field for each month of the year is shown in Fig. 12, and the average cosine efficiency of the mirror field for the year is 75.18 %. Using Eqs. (20)-(24), it can be calculated that the annual cosine efficiency of a fixed-tilt PV panel is approximately 65.97 % when the tilt angle is the local latitude.

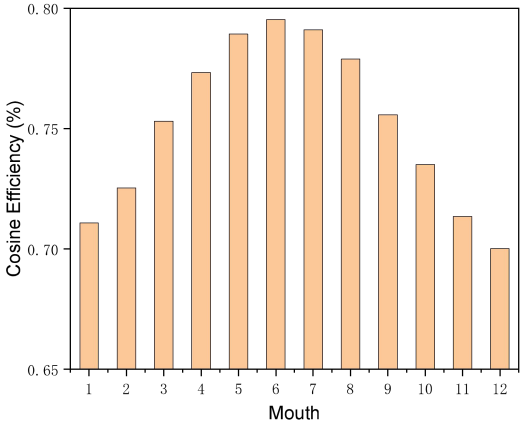

Figure 12: Monthly value of mirror field cosine efficiency

Using the introduction in section 3.3, the power production of the system can be obtained for monocrystalline solar cells at different moments of the year in the optimal band 500-900 nm. The full-year variation of power generation for tower-type T/PV hybrid system based on spectral beam splitting, fixed-tilt PV power generation system, and conventional tower-type solar thermal power generation system is shown in Figure 13.

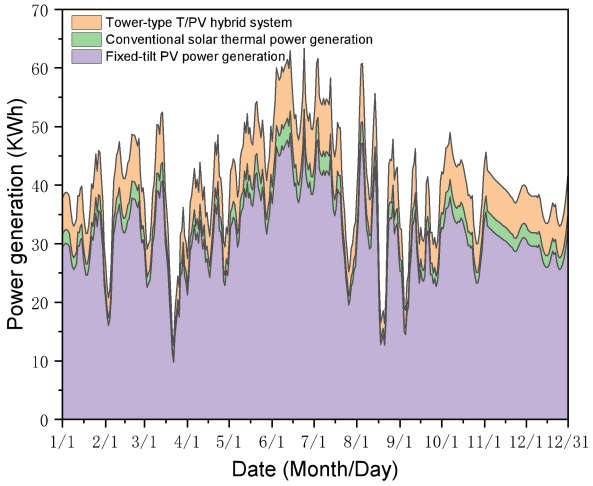

Figure 13: Daily power generation of the system throughout the year

The photothermal part of the tower-type T/PV hybrid system based on spectral beam splitting was obtained by bringing in parameters such as the average cosine efficiency, and the power generation efficiency of the photothermal part of the system after neglecting the shadow area was 17.83 %. The monthly average data of all calculated results in the tower-type T/PV hybrid system based on spectral beam splitting are shown in Table 2. The total power generation efficiency of the system is 21.32 %, which is higher than the power generation efficiency of both fixed-tilt PV power generation system and conventional tower-type solar thermal power generation system.

Table2 Comparison of thermodynamic analysis results of the tower-type T/PV hybrid system based on spectral beam splitting, fixed-tilt PV power generation system and conventional tower-type solar thermal power generation. system.

Parameters	Tower type T/PV hybrid system	fixed-tilt PV generation system	Conventional tower type system
Q_Z/kWh·m^{-2}	7696.64	7696.64	7696.64
Q_{in}/kWh·m^{-2}	5786.34	5077.47	5786.32
$Q_{PV,BS}$ or Q_{PV}/kWh·m^{-2}	2839.81	5786.34	—
$Q_{TH,BS}$ or Q_{TH}/kWh·m^{-2}	2946.53	—	5786.34
$P_{PV,BS}$ or P_{PV}/kWh·m^{-2}	941.91	1272.41	—
$P_{TH,BS}$ or P_{TH}/kWh·m^{-2}	698.91	—	1371.32
P_{total}/kWh·m^{-2}	1640.82	1272.41	1371.32
η_{PV}/%	12.24	16.53	—
η_{TE}/%	9.08	—	17.83
η_{SYS}/%	21.32	16.53	17.83

5. CONCLUSION

In this paper, we designed a spectral splitting glass that can completely transmit the specified wavelength band and completely reflect the other wavelength bands, and used it as a cover to lay on c-Si solar cells to form a spectral splitting PV module, and used the spectral splitting PV module to replace the heliostat in the tower power generation to obtain a new tower-type T/PV hybrid system based on spectral beam splitting. A preliminary model of no blocking mirror field distribution was established using the MUUEN algorithm, a mathematical model of the power generation of the system was constructed, and the model was analyzed optically and thermodynamically. The solar radiation data of a typical meteorological year in Lhasa were then used to predict the full-year power generation of the tower-type T/PV power generation system based on spectral beam splitting and compared with the fixed-tilt PV power generation system and conventional tower-type solar thermal power generation system. The results show that the proposed tower-based T/PV hybrid system based on spectral beam splitting has the highest power generation efficiency, which is 4.79 % and 3.49 % higher than the fixed-tilt PV power generation system and conventional tower-type solar thermal power generation system, respectively.

REFERENCES

[1] Li, Y.F. et al. (2022) 'Efficient and comprehensive photovoltaic/photothermal utilization technologies for solar energy', Power generation technology, 43(03), pp. 373-391.

[2] O'neill, S.(2021) 'Perovskite pushes solar cells to record efficiency', Engineering, 7(8), pp. 1037-1040.

[3] Ju, X. et al. (2012) 'Numerical analysis and optimization of a spectrum splitting concentration photovoltaic-thermoelectric hybrid system', Solar energy, 86(6), pp. 1941-1954.

[4] Zhang, F.(2019) 'Modulation and related mechanism of dislocations in cast quasi-single crystalline silicos', China: Zhejiang University.

[5] Ju, X. et al. (2017) 'A review of the concentrated photovoltaic/thermal (CPVT) hybrid solar systems based on the spectral beam splitting technology', Applied energy，187, pp. 534–563.

[6] Mahmoudinezhad, S. et al. (2022) 'Experimental investigation on spectrum beam splitting photovoltaic-thermoelectric generator under moderate solar concentrations', Energy, 238, pp. 121988.

[7] Widyolar, B. Jiang, L. Winston, R.(2018) 'Spectral beam splitting in hybrid PV/T parabolic trough systems for power generation', Applied energy, 209, pp. 236-250.

[8] Jiang, S. et al. (2010) 'Optical modeling for a two-stage parabolic trough concentrating photovoltaic/thermal system using spectral beam splitting technology', Solar energy materials and solar cells, 94(10), pp. 1686-1696.

[9] Liu Y. et al. (2010) 'Thermodynamic and optical analysis for a CPV/T hybrid system with beam splitter and fully tracked linear fresnel reflector concentrator utilizing sloped panels', Solar energy, 103, pp. 191-199.

[10] Segal, A. Epstein, M. Yogev, A.(2004) 'Hybrid concentrated photovoltaic and thermal power conversion at different spectral bands', Solar energy, 76(5), pp. 591-601.

[11] Wang G. et al. (2010) 'Thermodynamic and optical analyses of a hybrid solar CPV/T system with high solar concentrating uniformity based on spectral beam splitting technology', Energy,166, pp. 256-266.

[12] Siala, F.M.F. Elayeb, M.E.(2001) 'Mathematical formulation of a graphical method for a no-blocking heliostat field layout', Renewable energy, 23(1), pp. 77-92.

[13] Collado, F.J. Turégano, J.A.(1989) 'Calculation of the annual thermal energy supplied by a defined heliostat field', Solar energy, 42(2), pp. 149-165.

[14] Barberena J G. et al. (2016) 'State-of-the-art of heliostat field layout algorithms and their comparison', Energy procedia, 93, pp. 31-38.

[15] Wang, B.T.(2022) 'Study on solar spectral beam splitting photovoltaic/concentrated solar thermal system', China: Northeast Electric Power University.

[16] Xie F.(2013) 'Optical simulation of heliostat field in solar tower power system and its applkication', China: Zhejiang University.

[17] Stine, W.B. Geyer, M.(2001) Power from the sun.

Available at: http://powerfromthesun.net/index.html (Accessed: 9 June 2022)

[18] Yao, L.S.(2019) 'Estimation of power generation of solar power tower plants', Shanghai energy saving, 12, pp. 974-979.

[19] ASTM international. (2012) Standard tables for reference solar spectral irradiances：direct normal and hemispherical on 37° tilted surface. Available at: https://www.astm.org/g0173-03r12.html (Accessed: 21 September 2022)

[20] Green, M.A. et al. (2013) 'Solar cell efficiency tables (Version 42)', Progress in photovoltaics: research and applications,21, pp. 827-837.

[21] GREEN M A. et al. (2021) 'Solar cell efficiency tables (Version 58)', Progress in photovoltaics: research and applications, 29, pp. 657–667.